New Journal of Physics
An Institute of Physics and Deutsche Physikalische Gesellschaft Journal

Structural relaxation and mode coupling in a non-glassforming liquid: depolarized light scattering in benzene

Sabine Wiebel[1] **and Joachim Wuttke**[1,2]†

[1] Physik-Department E13, Technische Universität München, 85747 Garching, Germany

[2] Siemens AG, ICN ON RD AT 1, Hofmannstr. 51, 81359 München, Germany

E-mail: jwuttke@ph.tum.de

URL: http://www.e13.physik.tu-muenchen.de/Wuttke

New Journal of Physics **4** (2002) 56.1–56.17 (http://www.njp.org/)

Received 23 April 2002, in final form 21 June 2002

Published 31 July 2002

Abstract. We have measured depolarized light scattering in liquid benzene over the whole accessible temperature range and over four decades in frequency. Between 40 and 180 GHz we find a susceptibility peak due to structural relaxation. This peak shows stretching and time–temperature scaling as known from α relaxation in glass-forming materials. A simple mode-coupling model provides consistent fits of the entire data set. These qualitative and quantitative results show that structural relaxation in ordinary liquids and α relaxation in glass-forming materials are one and the same physical process. Thus, a deeper understanding of equilibrium liquids is reached by applying concepts that were originally developed in the context of glass-transition research.

1. Motivation

On short time scales, all liquids show solid-like elasticity. This has been impressively illustrated by Brillouin scattering of x-rays [1]: on a THz scale, sound propagates in water with almost the same speed as in ice, more than twice as fast as on the kHz or MHz scale of conventional ultrasonic measurements. Such a cross-over goes along with a decay of structural correlations; it is called *relaxation*, and more specifically α relaxation when it leads from solid-like to liquid-like response (correlations decaying to zero).

When a liquid can be supercooled far enough, α relaxation becomes critically slow, so that the material ultimately becomes a glass. The dynamics of glass-forming liquids has been

† Author to whom any correspondence should be addressed.

1367-2630/02/000056+17$30.00

studied in great detail. Stretching and time–temperature scaling have been identified as generic properties of α relaxation. Additional scaling laws have been uncovered by a mode-coupling theory (MCT). Originally proposed as a theory of the glass transition, MCT is now generally recognized to offer a unified description of microscopic and relaxational motion at comparatively high temperatures where α relaxation occurs on a GHz scale.

In experiments undertaken in both the supercooled and the normal liquid phase, α relaxation and mode-coupling dynamics are found to evolve continuously across the melting point of the concurrent crystalline phase: on a GHz–THz scale, the molecular dynamics seems to be insensitive to whether the liquid's state is thermodynamically stable or not. This leads us to the hypothesis that the molecular dynamics in the normal liquid state will be insensitive to whether the liquid can be supercooled or not. A pioneering paper on water [2], studies of metallic melts [3, 4], and our own experiments on several molecular liquids suggest that indeed α relaxation and mode-coupling effects also occur in liquids that cannot be supercooled into a glass.

For a more detailed test of our hypothesis, we now study one such liquid in depth. We choose benzene, which presents the following advantages:

(i) the molecule is structurally very simple and highly symmetric;
(ii) it is stiff on all relevant time or frequency scales†;
(iii) many often studied glass formers are structurally related to benzene;
(iv) benzene is an excellent light scatterer.

To investigate the dynamics of benzene over a wide dynamic range, we have used depolarized light scattering. A neutron scattering study is currently under way and will be published later; preliminary results support the conclusions we draw from light-scattering.

2. Context and theory

2.1. α relaxation

In zeroth approximation, relaxation may be modelled by an exponential decay of correlations. This ansatz goes back to Maxwell's theory of viscoelasticity; it has been elaborated for dielectric response by Debye [6]. The underlying physics is mean-field like: one considers thermal motion of an individual molecule upon which all the other molecules exert just a constant friction.

However, in glass-forming liquids α relaxation is found to be *stretched*: it is spread much more than an exponential decay in time or a Lorentz line (in our context: a Debye resonance) in frequency. Popular fit functions assume a fractional time or frequency dependence, as in Kohlrausch's stretched exponential

$$\Phi_{\mathrm{K}}(t) \propto \exp\left[-(t/\tau)^{\beta}\right], \tag{1}$$

or in the Cole–Davidson susceptibility

$$\chi_{\mathrm{CD}}(\nu) \propto (1 + \mathrm{i}2\pi\nu\tau)^{-\beta} - 1. \tag{2}$$

While the relaxation time τ depends strongly on the temperature T, the exponents β_{K} or β_{CD} vary only weakly. This can be seen as a consequence of *time–temperature scaling*: in a good first approximation, α relaxation has the form

$$\Phi(t;T) \simeq \hat{\Phi}(t/\tau(T)). \tag{3}$$

† The vibrational spectrum of benzene starts with an E_u^+ out-of-plane mode at 12.14 THz, see [5].

Towards high temperatures, this scaling law has an obvious limitation: α relaxation can never become faster than the temperature-independent microscopic modes. Indeed, on heating glass-forming materials towards the boiling point the curves $\log \tau$ versus T become flatter and flatter, so that τ approaches, but never reaches the intrinsic time scale of microscopic motion [7]. Depolarized light scattering in molecular liquids could clearly resolve an α peak and confirm its scaling up to temperatures far in the normal liquid phase [8, 9].

2.2. Relaxation in simple liquids

Historically, relaxation in simple liquids (on a THz scale), and α relaxation in highly viscous liquids (originally measured mostly on Hz–MHz scales) have long been seen as two genuinely different processes (see [10], page 260). In the most simple monatomic liquids like argon or sodium, on which theory-oriented textbooks [10]–[12] concentrate, characteristic relaxation times are of the order of 10^{-13}–10^{-12} s, which is not much longer than the mean time between collisions.† Under such circumstances relaxation is closely mingled with microscopic motion, and it is impossible to obtain isolated experimental information on relaxation alone. On the other hand, results of scattering experiments and molecular dynamics simulations cannot be understood without taking into account relaxation. Therefore, experimental data are usually fitted by theoretical expressions that contain memory kernels built upon an *ad hoc* model of relaxation.

Such fits, however, are rather insensitive to the functional form of the memory kernel, and therefore one seldom went beyond assuming simple exponential relaxation. In some cases, when fits were judged unsatisfactory, a sum of two exponentials was used (see [10], page 291); this approach, though admittedly arbitrary, has recently been revived in the analysis of x-ray Brillouin scattering on liquid metals [13]–[15].

In the investigation of glass-forming liquids this double-exponential approach has long been overcome by formulæ like (1) or (2). Today, after α relaxation has been observed across the melting point and up to a GHz–THz scale, it is no longer justified to consider relaxation in glass-forming materials and relaxation in ordinary liquids as two different physical processes. So we are led to suspect that the stretching and scaling properties of α relaxation hold in principle even in argon and sodium, although an experimental verification will be extremely difficult.‡

For the time being we prefer to investigate a molecular, non-glassforming liquid, benzene, which in a sense is intermediate between simple monatomics on the one side and molecular glass formers on the other side: the benzene molecule is small and highly symmetric, in contrast to glass-forming liquids which necessarily have a more complicated structure as to prevent crystallization. Yet we will find structural relaxation in benzene to be slow enough to allow for a direct, unambiguous observation of its stretching.

2.3. Mode-coupling theory

As mentioned in the beginning, MCT [17, 18] provides a unified description of α relaxation and low-frequency vibrations. It is a microscopic theory, formulated as function of wavenumber q

† 1.3×10^{-13} s for liquid argon, see [12].

‡ In the study of glass-forming liquids one has also learned that α relaxation alone is not sufficient to explain the damping of hydrodynamic modes; a physically meaningful relaxation kernel can only be constructed if one already possesses a rather complete knowledge of the microscopic dynamics, see [16].

and time t, and built upon the static structure factor $S(q)$ and the density correlation function $\Phi_q(t) = S(q,t)/S(q)$. It starts with the formally exact equation of motion

$$0 = \Omega_q^{-2}\ddot{\Phi}_q(t) + \Phi_q(t) + \int_0^t \mathrm{d}t'\, M_q(t-t')\dot{\Phi}_q(t'). \tag{4}$$

The memory kernel $M_q(t)$ contains fast and slow fluctuations, $M_q(t) \simeq M_q'(t) + m_q(t)$. The fast component, approximated as $M_q'(t) \simeq \gamma_q\delta(t)$, can be shown to be irrelevant for the long-time behaviour.

The basic idea of MCT is now to expand the slow fluctuations $m_q(t)$ in polynomials of density fluctuations, and then to factorize all terms into pair correlations. In lowest order one obtains the bilinear functional

$$m_q\{\Phi(t)\} = \sum_{\boldsymbol{p}+\boldsymbol{k}=\boldsymbol{q}} V_{\boldsymbol{qpk}}\Phi_p(t)\,\Phi_k(t). \tag{5}$$

The coupling coefficients $V_{\boldsymbol{qpk}}$ can be derived from the static structure factor $S(q)$; as $S(q)$, they vary slowly with state variables like temperature T or pressure P. In this way the dynamics is completely determined by a closed set of integro-differential equations. Depending on the numeric values of $V_{\boldsymbol{qpk}}$, the $\Phi_q(t)$ either decay to zero or arrest at finite values. The border line $T_\mathrm{c}(P)$ which separates these two cases has been called the *ideal glass transition*.

For $T < T_\mathrm{c}$, the density correlations arrest at a finite Debye–Waller factor $\Phi_q(t \to \infty) = f_q(T)$, as expected for a glass. On the liquid side, with $T > T_\mathrm{c}$, the $\Phi_q(t)$ slow down on approaching a plateau $f_q(T)$, but ultimately they decay to $\Phi_q(t \to \infty) = 0$ in a process which is easily identified as α relaxation. Since the derivatives $\ddot{\Phi}_q(t)$ become negligible at long times, equation (4) immediately reproduces the time–temperature scaling (3), with the corollary that the line shape of $\hat{\Phi}_q$ may vary with q. To first order, solutions of MCT equations are consistent with the Kohlrausch asymptote (1).

On cooling towards T_c, α relaxation times are predicted to diverge with a fractional power law in $T - T_\mathrm{c}$. A comparison with measured relaxation times and viscosities [19] shows that such a divergence does *not* correctly describe the glass transition.† Instead, T_c is found to describe a cross-over that is typically located 15–20% *above* the conventional glass transition temperature T_g: while the density–density coupling of equation (5) becomes ineffective at T_c, other transport mechanisms, not covered by the theory, remain active at lower temperatures. This interpretation of T_c is supported by various other experimental indications of a cross-over.‡

In liquids to which MCT has been applied in the past, the cross-over occurs at shear viscosities of the order of 10^1–10^3 poise [19]. We note that this is much closer to the viscosity of, say, water at room temperature (about 10^{-2} poise) than to the glass transition (which, according to widespread convention, occurs at 10^{13} poise). We note also that the dynamic predictions of MCT are expected to work best not in the immediate vicinity of T_c, but at somewhat higher temperatures where the concurrence of low-temperature transport processes can be neglected.

† We restrict ourselves to Newtonian liquids. In Brownian liquids, as formed e.g. by colloidal suspensions, the ergodic–nonergodic transition is well described by MCT, see [20].

‡ The Stokes–Einstein relation which is supposed to connect self diffusion and shear viscosity is found to break down on cooling below about T_c, see [21]. The temperature at which fast β relaxation dies out seems to coincide with T_c, see [22]. Empirical formulæ fail to describe the temperature dependence of viscosity simultaneously from the glass transition up to the normal liquid phase. Several methods of data reduction indicate that there are two different dynamic regimes, separated by T_c: see section 2.3 in [18], and [53].

This suggests that MCT should be tested as a theory that describes the dynamics of glass-forming liquids at rather low viscosities, far above the glass transition, in a slightly supercooled or thermodynamically stable state. In this paper we want to show that the restriction to *glass-forming* liquids can be omitted altogether.

2.4. Applying mode coupling to real-life liquids

Taken literally, equations (4) and (5) assume a liquid composed of identical, spherical, and stiff particles: only in this case all interactions between the particles can be derived from $S(q)$. Extending the theory to mixtures is straightforward [23, 24], but including orientational and intramolecular degrees of freedom poses extreme difficulties: the notational and calculational efforts required by models so simple as a liquid made of linear molecules [25, 26], or a dilute solution of linear molecules in spheres [27, 28] are intimidating. Thus, a MCT of molecular liquids is presently not available.

On the other hand, the time and temperature dependence of MCT solutions is insensitive to most of the structural information hidden in $V_{\boldsymbol{qpk}}$. Taking into account orientational or intramolecular degrees of freedom may lead to new classes of solutions, but at least in some types of molecular liquids the fundamental mathematical structure of equations (4) and (5) will remain dominant.

In such cases, MCT solutions can be characterized by quite few parameters. Close to T_c, the analytical expansions of $\Phi_q(t) - f_q$ depends in lowest order on just one nontrivial line shape parameter λ. Complete time correlation functions can be generated by numeric solutions of very simple MCT models: In the minimal F_{12} model [29], just one correlator $\Phi(t)$ and two coupling coefficients in

$$m(t) = v_1\Phi(t) + v_2[\Phi(t)]^2 \tag{6}$$

are sufficient to obtain relaxational stretching and the ideal glass transition. With just one more correlator, $\Phi_s(t)$, one can generate spectra with arbitrary α relaxation strengths f_q^s: a bilinear memory kernel [30, 31]†

$$m_s(t) = v_s\Phi(t)\Phi_s(t) \tag{7}$$

couples $\Phi_s(t)$ to $\Phi(t)$, whereas $\Phi(t)$ does not depend on $\Phi_s(t)$.

The so-defined two-correlator F_{12} model is a physically meaningful tool for fitting experimental data. As such it has already been successfully employed in several studies of glass-forming liquids [32]–[35]; the theoretical background is explained especially in [35]. A detailed numeric study has confirmed the stability of such fits [36].

3. Light scattering measurements

Benzene ($T_m = 279$ K, $T_b = 353$ K) was bought from Sigma Aldrich (99.9% puriss. p.a.), unpacked under inert gas and sealed into a Duran cuvette. To our surprise, the sample could

† Under the very name 'mode-coupling theory' the kernel (7) has already been employed in classical studies of tagged-particle motion in simple liquids [12, 54, 55]. However, in those studies the mode-coupling approach was only used for $\Phi_s(q,t)$, whereas the $\Phi(q,t)$ to which they couple were typically discussed in terms of exponential memory kernels. A self-consistent ansatz for $\Phi(t)$ was first proposed in the context of the glass transition [30, 56], and only through the experience with glass-forming systems we were led to apply it to the simple liquid benzene.

be supercooled to 258 K where it remained liquid for several hours. Data were taken at seven temperatures between 258 and 352 K.

Light scattering experiments were performed using a grating double monochromator U 1000 and a six-pass Sandercock–Fabry–Perot tandem interferometer. In order to achieve stable operation at maximum resolution, both instruments are placed in insulating housings with active temperature control. The optics around the interferometer has been modified as described previously [37, 38]. Depending on the spectral range, the interferometer is used in series with an interference filter of either 150 or 1000 GHz bandwidth that suppresses higher-order transmission leaks of the tandem interferometer [39]–[41] below 3% or better. The filters are maintained at constant temperature. To account for any drift, the instrument function is redetermined periodically by automatic white-light scans.

In the present experiment, the slits of the monochromator are set to 30–60–60–30 μm, resulting in a resolution (FWHM) of 7.5 GHz; data are only used above 200 GHz. The interferometer is operated with mirror spacings of 0.4, 2.8, and 16.3 mm, corresponding to free spectral ranges of 375, 54, and 9.2 GHz; some additional data were taken with 7.5 mm (20 GHz).

On both spectrometers, a near-backscattering geometry (172°) is used to minimize scattering from transverse modes. In depolarized (HV) interferometer measurements, the usual leakage from the acoustic modes is seen; these lines are about a hundred times weaker than in polarized (VV) scattering, but still up to about three times stronger than the continuous HV spectrum. Subtracting separately measured VV spectra†, we could completely remove the contamination from the HV data.

Intensity calibration is always a problem in light scattering. Best results were obtained by matching all data to the middle (54 GHz) spectral range of the interferometer. In this range intensities are reproduced after a full temperature cycle within about 3%. The temperature-dependent intensity mismatch of other spectral ranges is higher and attains up to 20%. Part of the problem may be due to distortions of the optical paths within the cryostat, which are particularly severe when the spectrometer is operated with small entrance opening. In the present study, intensities can also be estimated from the mode-coupling fits which are normalized by construction (see figure 3).

Finally, the spectra are multiplied with the detailed-balance factor,

$$\tilde{I}(\nu) = I(\nu)\exp(-h\nu/2k_{\mathrm{B}}T), \tag{8}$$

averaged over energy-gain and energy-loss side, and converted from intensity to susceptibility

$$\chi''_{\mathrm{ls}}(\nu) = \tilde{I}(\nu)/\tilde{n}(\nu) \tag{9}$$

with the symmetrized Bose factor

$$\tilde{n}(\nu) = \frac{1}{\exp(h\nu/2k_{\mathrm{B}}T) - \exp(-h\nu/2k_{\mathrm{B}}T)}. \tag{10}$$

In other molecular liquids, comparison with neutron scattering [37], [42]–[46] has shown that depolarized light scattering yields at least qualitatively a good representation of the dynamic susceptibility, and therefore we will interpret $\chi''_{\mathrm{ls}}(\nu)$ in very much the same way as a susceptibility from incoherent neutron scattering.

† We have not further analysed the VV spectra. Note, however, that we find a nontrivial sound dispersion: whereas up to some MHz the room-temperature sound velocity of benzene is about 1300 m s^{-1}, our VV Brillouin scattering data give about 1500 m s^{-1} at 5 GHz.

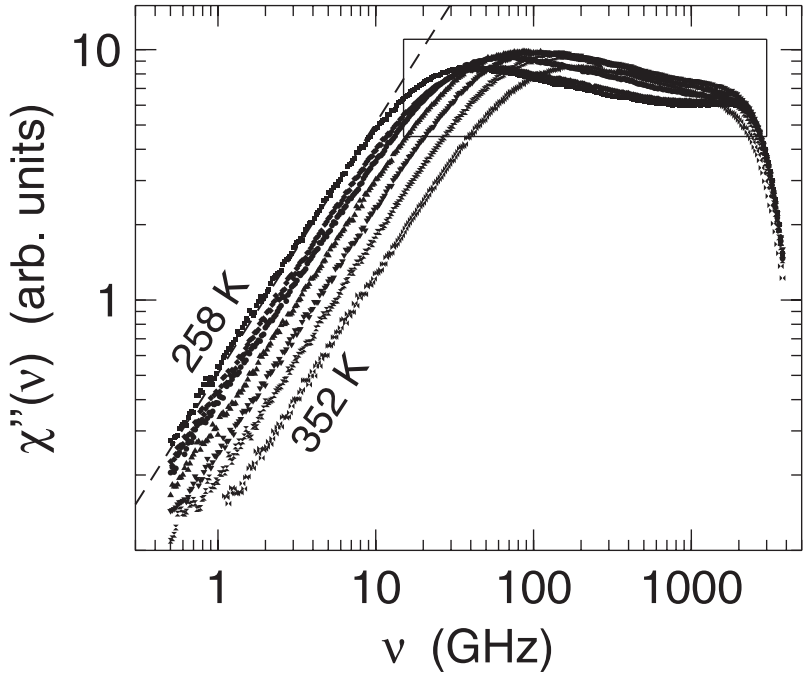

Figure 1. Susceptibilities of benzene measured by depolarized light scattering at temperatures $T = 258, 268, 279, 293, 310, 330$ and 352 K. In the low-frequency wing, one finds the white-noise slope ν^1, indicated by the dashed line. The nontrivial relaxational and microscopic dynamics inside the rectangular frame is shown on an enlarged scale in figure 2.

4. Data and analysis

4.1. Susceptibilities on logarithmic scales

Figure 1 shows susceptibilities from depolarized light scattering for seven temperatures between 258 and 352 K. In studies of glass-forming liquids, measuring susceptibilities over several decades and representing them on double-logarithmic scales were decisive steps in detecting nontrivial, stretched relaxation [47]. In the case of benzene, the same procedure, on the same absolute frequency scale, is less rewarding: too much of figure 1 is filled by an uninformative ν^1 white-noise wing.

Therefore we show the nontrivial part of our data in figure 2 on an enlarged scale: the strongly temperature-dependent dynamics between 15 GHz and 3 THz. With increasing frequency, the $\chi''(\nu)$ begin to deviate from the white-noise limit $\chi'' \propto \nu^1$, reaching a maximum between 40 and 180 GHz which we will ascribe to structural α relaxation. A comparatively flat region leads over to a shoulder at about 2 THz, above which the susceptibilities strongly decrease. Above 5 THz we find an extended gap; intramolecular excitations are only expected above 12 THz [5].

The whole scenario is compatible with the high-temperature limit of what has been observed in many glass-forming systems. We note that the picture does not change up to the highest accessible temperatures: little below the boiling point, the α peak is still separated by almost a decade in frequency from the vibrational shoulder.

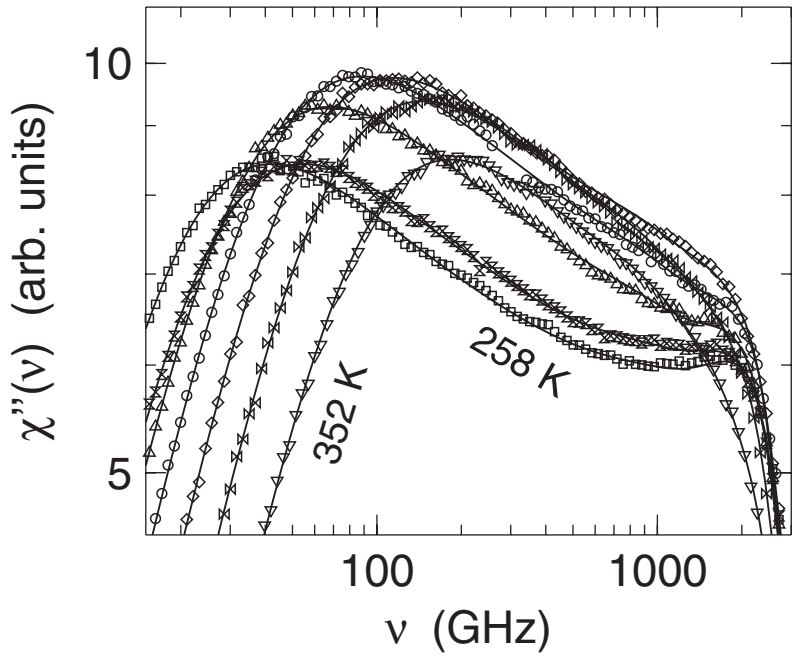

Figure 2. Enlargement of the intermediate frequency region of figure 1. Structural α relaxation leads to a peak between 40 and 180 GHz. The shoulder at about 2 THz is associated with microscopic ballistic motion. The flat cross-over between these two peaks is a signature of mode-coupling dynamics: the data cannot be explained as a simple superposition of α relaxation and harmonic short-time motion. Solid curves are fits with the mode-coupling two-correlator F_{12} model (see figure 3, sections 2.3 and 4.5 and table 1).

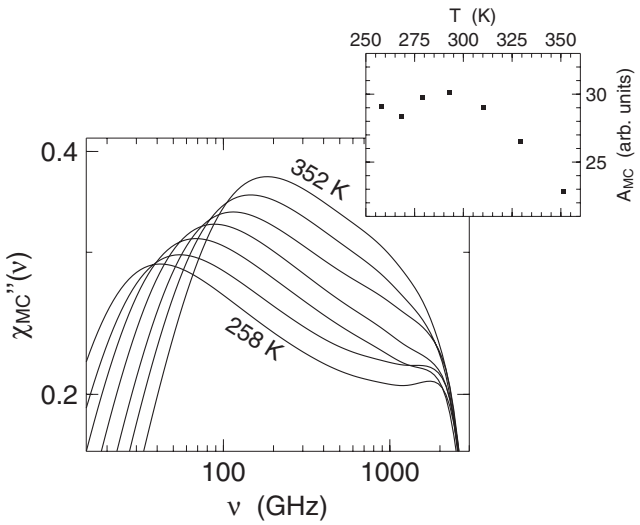

Figure 3. The curves in the main figure are identical to the mode-coupling fits of figure 2, except for being shown in absolute units, fulfilling the χ''/ν sum rule. The inset shows the amplitudes $A_{\mathrm{MC}}(T)$ by which these curves had to be multiplied in order to fit the experimental data; these amplitudes essentially represent the Pockel coefficient by which light scattering couples to the microscopic dynamics.

Table 1. Parameters of the two-correlator F_{12} model, as obtained from the least-squares fits shown in figure 2. Note that v_1, v_2, and v_s are dimensionless, whereas Ω, γ, and γ_s are given in GHz. The amplitude A_{MC} is in the arbitrary units of our depolarized light scattering experiment. The eighth parameter, $\Omega_s/2\pi = 1000$ GHz, was kept fixed.

T(K)	v_1	v_2	v_s	$\Omega/2\pi$	$\gamma/2\pi$	$\gamma_s/2\pi$	A_{MC}
258	0.7510	1.172	2.96	821.7	1283	2025	29.07
268	0.7742	1.063	2.845	892.3	1337	1939	28.31
279	0.7380	1.054	2.581	803.7	1086	2089	29.78
293	0.7490	0.988	2.569	905.5	1027	1939	30.09
310	0.7297	0.9781	2.403	971.4	1030	1795	28.99
330	0.7159	0.9682	2.179	983.5	918.1	1830	26.54
352	0.6957	0.9840	2.174	1115	785.4	1674	22.82

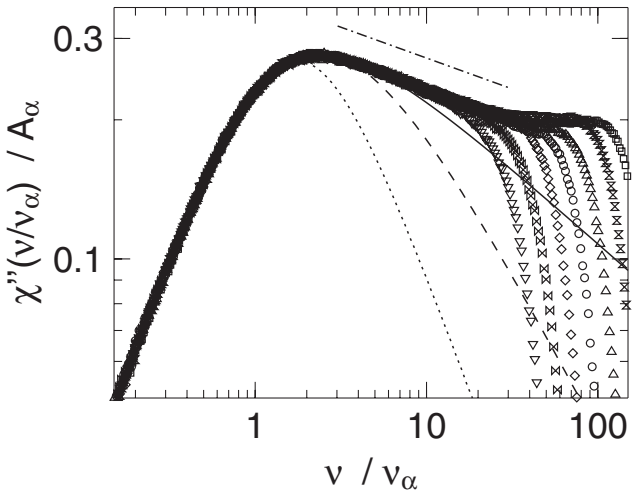

Figure 4. Master curve, constructed by rescaling the light scattering data of all seven temperatures (symbols as in figure 2) to a common α peak. The peak is more stretched than any of the usual fit formulæ is able to describe: a Lorentzian, motivated by the viscoelastic theory of Maxwell and Debye, is completely inadequate (dotted curve). Kohlrausch's stretched exponential (equation (1) with $\beta_K = 0.73$, dashed curve) and the Cole–Davidson function (equation (2), straight line) hold at least up to above the maximum of the peak. At higher frequencies, the extremely flat wing approximately follows a power law ν^{-b} with $b \simeq 0.13$ (dash–dotted line).

4.2. Absolute intensities

The temperature dependence of the scattering intensity is surprising: the height of the α peak increases by about 15% on heating from 258 to 293 K; then it falls back and reaches at 352 K about the starting level. The apparent anharmonicity in the high-temperature, high-frequency limit is unexpectedly pronounced, though a similar trend has been observed in several other liquids.

To disentangle possible causes of these anomalies, we take advantage of mode-coupling fits. The physical meaning of these fits will be discussed later (section 4.5); for the moment we take them just as a smooth parametrization of the measured data—with one specific advantage: Since the mode-coupling susceptibilities are obtained by Fourier transformation of the derivative of a time correlation function, they obey the $\chi''(\nu)/\nu$ sum rule by construction. Therefore we can take them as representing our light scattering data in absolute normalization.

Resulting curves are shown in figure 3: they are strictly identical to the mode-coupling fits included in figure 2—except that the latter are multiplied by an amplitude A_{MC} to adjust them to the arbitrary experimental intensity. Thanks to the intrinsic normalization, figure 3 shows a highly regular temperature dependence. In particular, we no longer see indications for a softening of the microscopic excitation spectrum at high temperatures: in the high-frequency wing, up to the boiling point all susceptibilities coincide, as expected for harmonic motion. The α peak height increases steadily with T; only between 1 and 2 THz are small experimental imperfections visible.

The temperature dependence of A_{MC} is shown in the inset of figure 3. Up to 293 K the $A_{\mathrm{MC}}(T)$ scatter somehow, then they decrease systematically towards about 75% of the low-temperature average. A similar decrease of depolarized scattering intensity has been observed in many other liquids. However, lacking a means of absolute normalization, it was never clear whether this decrease reflected a property of the sample or of the scattering process. Instabilities of the experimental setup added to the difficulty. It now appears that the decrease of scattering intensities at high temperatures in figure 3 is *not* due to the sample dynamics; it rather appears that $A_{\mathrm{MC}}(T)$ reveals a temperature variation of the Pockel coefficient that couples light scattering to the microscopic dynamics.

4.3. α relaxation

For a quantitative analysis of α relaxation, we first test time–temperature superposition. Using the frequency-space representation of equation (3), and allowing for a temperature dependent amplitude, we rescale our data onto a master curve. Figure 4 shows that the line shape is independent of temperature up to at least five times the peak frequency.

The α peak is obviously stretched, as can be seen by comparison to a Debye curve (dotted curve). The data are far better described by one of the empirical expressions (1) or (2). The Fourier transform of the Kohlrausch stretched exponential (1) fits the master curve up to about twice the peak frequency (dashed curve) with a stretching exponent $\beta_{\mathrm{K}} \simeq 0.73$.

The Cole–Davidson function (2) with $\beta_{\mathrm{CD}} \simeq 0.33$ describes the master curve to even higher frequencies (solid line). Consequently, we use Cole–Davidson fits to determine the mean relaxation time

$$\langle\tau\rangle = \int \mathrm{d}t\, \Phi(t)/\Phi(0) = \beta_{\mathrm{CD}}\tau, \tag{11}$$

which in turn is used in the iterative construction of the master curve.

None of the empirical fit functions is able to fully describe the extremely flat high-frequency wing of the α peak. For about one decade, this wing roughly follows a power law ν^{-b} (dash–dotted line in figure 4). The exponent is about $b \simeq 0.13$, the precise value depending on the choice of the frequency range. Such a power law is reminiscent of MCT, though it should not be taken literally as an MCT asymptote (see section 4.5 below).

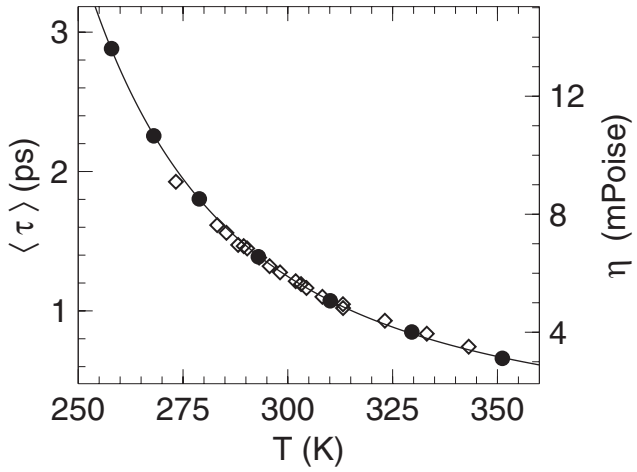

Figure 5. Mean relaxation times $\langle\tau\rangle$ as obtained from Cole–Davidson fits to the light-scattering susceptibility in the α relaxation region (●, left scale). Solid curves are fits by the Vogel–Fulcher function (equation (12), section 4.4). The temperature dependence agrees in first order with that of the shear viscosity η (⋄, literature data [48], right scale).

4.4. Relaxation times

In a next step, we investigate the temperature dependence of the mean relaxation time $\langle\tau\rangle$, as determined from the Cole–Davidson fits (11).

In figure 5, $\langle\tau\rangle$ is plotted as a function of temperature and compared with the shear viscosity η. In a good first approximation, $\langle\tau\rangle$ and η show the same temperature dependence. This completes the demonstration that the susceptibility peak under study is indeed due to α relaxation, in the same sense as in any glass-forming liquid. The approximate proportionality $\langle\tau\rangle \propto \eta$ can be used to extend available viscosity data [48] by more than 15 K into the supercooled phase, and by 9 K towards the boiling point.

Furthermore, figure 5 shows a Vogel–Fulcher fit

$$\langle\tau\rangle \propto \exp\left(-\frac{E_0}{T-T_0}\right) \tag{12}$$

to the mean relaxation times, with $T_0 = 94.2$ K and $E_0 = 650.6$ K. We abstain from any physical interpretation, since several decades in $\langle\tau\rangle$ are needed for a meaningful verification of (12); we just employ the fit as a tool for a more detailed comparison of $\langle\tau\rangle$ and η.

This comparison is performed in figures 6(a) and (b) where we divide either η or η/T by the Vogel–Fulcher estimate of $\langle\tau\rangle$. A proportionality $\langle\tau\rangle \propto \eta/T$ is suggested by the Stokes–Einstein relation $D \propto T/\eta$: when the diffusion constant D is determined from a time correlation function,

$$\Phi(t) \propto \exp(-Dq^2t), \tag{13}$$

one has $\langle\tau\rangle \propto D^{-1}$ and thus $\langle\tau\rangle \propto \eta/T$. Of course the stretched α relaxation in benzene is not correctly described by equation (13). Therefore the theoretical grounds for assuming $\langle\tau\rangle \propto \eta/T$ are rather weak.

And indeed, figure 6 shows that $\langle\tau\rangle$ is not proportional to η/T, nor to η, but something in between. Such a temperature dependence has been reported at least once before: in a neutron

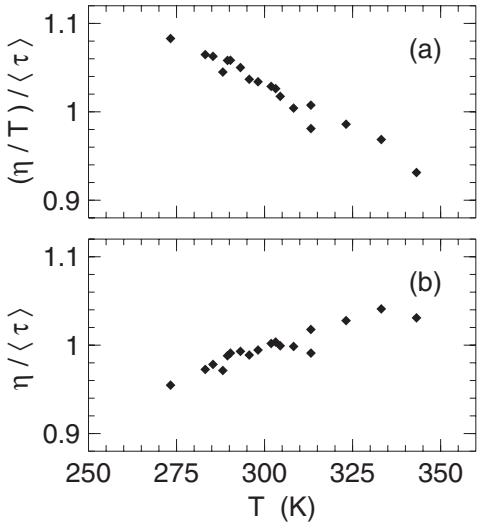

Figure 6. For a more detailed comparison of η and $\langle\tau\rangle$, we eliminate their common first-order temperature dependence by plotting quotients. Shear viscosity data are the same as in figure 5; the relaxation times $\langle\tau\rangle$ are interpolated to the corresponding temperatures by means of the Vogel–Fulcher fit. The comparison (a) of $\langle\tau\rangle$ and η/T is motivated by the Stokes–Einstein relation. However, (b) shows that $\langle\tau\rangle$ agrees slightly better with η than with η/T. Both plots are in arbitrary units†.

spin-echo experiment on the high-temperature dynamics of glycerol [49]. We therefore conclude: the mean relaxation time observed by scattering shows the same temperature dependence as the shear viscosity—up to a weakly temperature-dependent prefactor which at present no theory is able to predict.

4.5. Mode-coupling fits

We now extend our analysis beyond the α peak, considering the full experimental frequency scale up to some THz. The theoretical reference is given by MCT. MCT is perfectly compatible with the scaling properties of α relaxation obtained in the two preceding sections. Additionally, MCT predicts that α relaxation has a rather flat high-frequency wing which leads over to the microscopic molecular dynamics. This is just what we see in figures 2–4.

In glass-forming liquids, mode-coupling analysis usually concentrates on a scaling regime, designated as fast β relaxation, which is located between α peak and microscopic frequencies. When the α relaxation becomes sufficiently slow, the dynamic susceptibility passes through a minimum, and for frequencies around this minimum simple asymptotic power laws are predicted. In benzene we find a susceptibility minimum at the two lowest temperatures. This once again supports qualitative accord with an MCT scenario, though the β relaxation regime is not sufficiently developed to allow a scaling analysis.

† Arbitrary units were chosen in order to keep the figure as light as possible. In order to obtain $\eta/T/\langle\tau\rangle$ or $\eta/\langle\tau\rangle$ in absolute values, multiply in figure 6(a) with 15.2×10^{6} poise $\mathrm{K}^{-1}\,\mathrm{s}^{-1}$, and in figure 6(b) with 4.67×10^{9} poise s^{-1}.

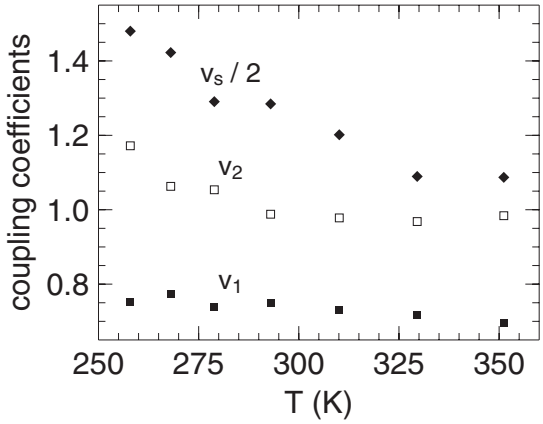

Figure 7. Coupling coefficients used in the schematic mode-coupling fits (figures 2 and 3, and section 4.5). Numeric values are also given in table 1. The coefficients v_1 and v_2 of equation (6) control the intrinsic dynamics of the liquid, represented by the correlation function $\Phi(t)$; the slave correlator $\Phi_s(t)$, which represents the experimental observable, couples to $\Phi(t)$ via v_s (equation (7)). In agreement with the spirit of MCT, we find decreasing coefficients with increasing temperature.

The approximate power law ν^{-b} (section 4.3, figure 4) in the high-frequency wing of the α peak is of the low-frequency asymptote of fast β relaxation; however, the exponent $b \simeq 0.13$ implies a line shape parameter $\lambda \simeq 0.98$ which, though formally allowed, is highly unlikely to represent the true asymptotic value, which whenever reliably determined has been found to fall into the range of about 0.65–0.8. We therefore think that ν^{-b} represents not more than a transient: somehow related to the scaling properties of MCT, but not representing an analytical asymptote of the β minimum.

Therefore, we use numerical instead of asymptotic solutions of MCT. Specifically, we use the two-correlator F_{12} model, introduced in section 2.3, which is defined by the equation of motion (4) (with the set $\{\Phi_q\}$ replaced by the pair $\{\Phi, \Phi_s\}$) and the memory kernels (6), (7). While $\Phi(t)$ models the intrinsic dynamics of the system, $\Phi_s(t)$ shall be interpreted as the correlation function observed by depolarized light scattering.

The model contains seven parameters: two frequencies Ω, Ω_s characterizing ballistic short-time motion, two damping coefficients γ, γ_s representing fast contributions to the memory kernel in equation (4), and three coupling coefficients v_1, v_2 and v_s. These parameters are all expected to vary smoothly and monotonously with temperature. An eighth parameter, the amplitude A_{MC}, is not part of the model, but needed to adjust it to the arbitrary experimental intensity scale; these amplitudes have already been discussed above (section 4.2, figure 3).

The inner loop of the fit routine calculates $\Phi(t)$ and $\Phi_s(t)$ by iteratively solving equation (4) in the time domain [50]–[52]. Then $\Phi_s(t)$ is converted into a susceptibility by blockwise Fourier transform, using the Filon method. The so-obtained $\chi_s''(\nu)$ are fitted to the experimental data.

This procedure is performed independently for each of the seven measured temperatures. In an attempt to reduce the number of free parameters we find that the microsopic frequency

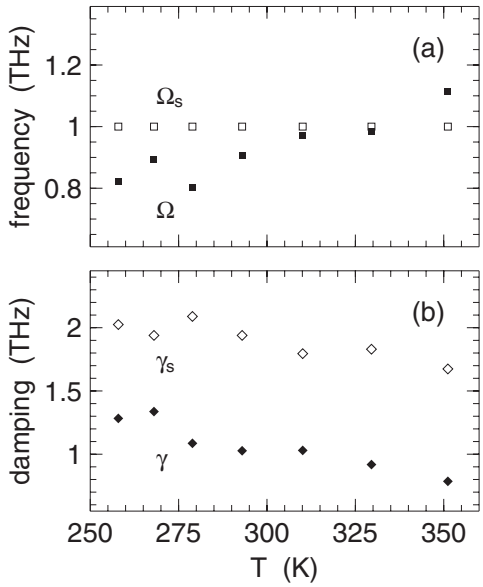

Figure 8. In continuation of figure 7, the remaining parameters of the mode-coupling fits are shown: (a) the microscopic frequencies Ω (full squares) and Ω_s (open squares, kept fixed) of equation (4), and (b) the damping coefficients γ (full diamonds) and γ_s (open diamonds) representing the rapidly decaying part $M'_q(t)$ of the memory kernel. Since we are using THz units, the figure shows strictly speaking $\Omega/2\pi$ etc.

of the slave correlator can be kept at a constant value $\Omega_s/2\pi = 1000$ GHz. All other parameters are found to show a weak, regular temperature dependence with only minor deviations from monotonicity, as can be seen in figures 7 and 8.† Values are also numerically given in table 1.

The time dependence of α relaxation is essentially given by the coupling coefficients v_1 and v_2. In figure 9 the values obtained from our fits are shown as points in a phase diagram. For large values of v_1 and v_2, the F_{12} model becomes a glass. The phase boundary corresponding to the idealized liquid–glass transition is indicated in the figure.

In benzene, the coupling coefficients fall clearly in the liquid phase; with decreasing temperature the glass-transition singularity is only a little approached. This correlates with the fact that the measured susceptibilities show only a very first onset of a fast β-relaxation minimum. For the same reason it would not be meaningful to use asymptotic scaling laws that are based on expansions in $T - T_c$. From the available v_1, v_2, it is not even possible to extrapolate a hypothetical trajectory by which benzene would approach the glass transition if it could be further supercooled. Therefore it is impossible to indicate a meaningful value of the asymptotic line shape parameter λ.

† In [32]–[34] all frequencies and damping constants could be kept independent of temperature. In our case, such a constraint leads to a significant deterioration of the mode-coupling fits. Probably, we are more sensitive to weak variations of the microscopic dynamics just because we are restricted to a high-temperature regime in which relaxational frequencies are much closer to the microscopic peak than in a deeply supercooled glass-forming liquid.

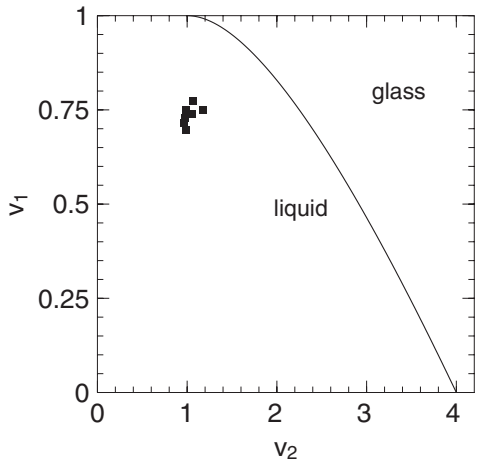

Figure 9. Mode-coupling coefficients v_1 and v_2 as in figure 7 in the phase diagram of the F_{12} model. The solid curve indicates the ideal glass-transition singularity. On cooling liquid benzene through its entire range of existence, this phase boundary is only a little approached.

5. Conclusion

We used depolarized light scattering to measure the dynamic susceptibility of liquid benzene. Four spectral ranges of two spectrometers were combined to cover frequencies from 0.5 GHz to several THz. White noise prevails up to 10 GHz (figure 1). Depending on temperature, a relaxational maximum is attained between 40 and 180 GHz. The high-frequency wing of this maximum is extremely flat, and extends up to about 2 THz. In the supercooled state, the susceptibility passes through a slight minimum around 1 THz (figures 2 and 3).

Such a broad relaxation pattern cannot be described by exponential memory functions that underlie conventional theories of simple liquids. Instead, our results look very similar to what has been observed in many glass-forming liquids. This confirms our starting hypothesis, and provides the basis for our quantitative data analysis.

As in glass-forming liquids, the relaxational α peak is stretched; it is even more stretched than the common fit formulæ are able to describe. Time–temperature scaling is obeyed with high precision and up to the boiling point, contradicting certain glass-transition theories which assume that α relaxation becomes Debye-like in the high-temperature limit (figure 4).

Within the accessible temperature range, the mean relaxation time $\langle\tau\rangle$ of benzene varies by more than a factor of 4, and it is roughly proportional to the shear viscosity η (figure 5). This accord is *not* improved by applying the Stokes–Einstein formula according to which $\langle\tau\rangle$ should go with η/T rather than η (figure 6). Implications are discussed in section 4.4.

Our observations are fully compatible with MCT. Originally, this theory attracted attention because of its ability to model a density-driven transition into a nonergodic state. Very soon, however, it became clear that this singularity does not describe glass formation. Instead, it is now generally recognized that MCT describes liquid dynamics at relatively low viscosities. In several studies of glass-forming liquids, fits were extended above the melting point of the concurrent crystalline phase, which was found to be irrelevant for the molecular dynamics under study. In

our present work, we push this evolution one step further by applying MCT to a liquid that can hardly be supercooled (actually, benzene *can* be supercooled by nearly 20 K, which came out as quite a surprise). In our experiment, we cover the full range of existence, up to 1 K below the boiling point.

In this temperature range, we can no longer apply the asymptotic expansions that are used in most MCT studies of glass-forming materials. Instead, we use numeric solutions of the full mode-coupling equations of motion. An elementary model with two correlators and three coupling coefficients is sufficient for a satisfactory fit to our full experimental data set. All parameters show a smooth, physically reasonable temperature dependence (figures 7 and 8). Previous mode-coupling studies on glass-forming samples mostly concentrated on the asymptotic predictions for fast β relaxation. A phase diagram makes clear that this scaling regime is not accessible in benzene (figure 9). In such a situation numeric solutions of a minimal mode-coupling model provide the most adequate description of dynamic susceptibilities on the GHz–THz scale of structural relaxation and microscopic motion.†

Acknowledgments

We thank M Goldammer, W Götze, H Schober, and W Petry for invaluable support. M Fuchs, M R Mayr, A P Singh and T Voigtmann showed us how to solve the F_{12} model. We acknowledge funding by the German DFG under project Me1958/3–1.

References

[1] Sette F *et al* 1996 *Phys. Rev. Lett.* **77** 83
[2] Sokolov A P, Hurst J and Quitmann D 1995 *Phys. Rev.* B **51** 12 865
[3] Meyer A *et al* 1998 *Phys. Rev. Lett.* **80** 4454
[4] Meyer A, Busch R and Schober H 1999 *Phys. Rev. Lett.* **83** 5027
[5] Sverdlov L M, Kovner M A and Krainov E P 1974 *Vibrational Spectra of Polyatomic Molecules* (New York: Wiley)
[6] Debye P 1929 *Polar Molecules* (New York: Dover)
[7] Angell C A 1997 *Polymer* **38** 6261
[8] Cummins H Z *et al* 1997 *Prog. Theor. Phys. Suppl.* **126** 21
[9] Wiedersich J, Surovtsev N V and Rössler E 2000 *J. Chem. Phys.* **113** 1143
[10] Boon J P and Yip S 1991 *Molecular Hydrodynamics* corrected reprint (New York: Dover)
[11] Hansen J P and McDonald I R 1986 *Theory of Simple Liquids* 2nd edn (London: Academic)
[12] Balucani U and Zoppi M 1994 *Dynamics of the Liquid State* (Oxford: Clarendon)
[13] Scopigno T, Balucani U, Ruocco G and Sette F 2000 *Phys. Rev. Lett.* **85** 4076
[14] Scopigno T, Balucani U, Ruocco G and Sette F 2000 *Phys. Rev.* E **63** 011210
[15] Scopigno T, Balucani U, Ruocco G and Sette F 2002 *Phys. Rev.* E **65** 031205
[16] Brodin A *et al* 2002 *Phys. Rev.* E **65** 05150
[17] Götze W 1991 *Liquids, Freezing and the Glass Transition (Les Houches, session LI)* ed J P Hansen, D Levesque and D Zinn-Justin (Amsterdam: North Holland)

† This does not mean that MCT tells the full story about the dynamics of benzene. The sound dispersion (see first footnote on p 1.3) for instance indicates that there are other, nontrivial relaxation processes on time scales below that of α relaxation. It seems plausible that these processes have to do with medium-range order; one could imagine that the disc-like benzene molecules assemble in form of liquid planes and piles. However, these processes are far too slow to interfere with the microscopic dynamics we have concentrated on.

[18] Götze W and Sjögren L 1992 *Rep. Prog. Phys.* **55** 241
[19] Taborek P, Kleiman R N and Bishop D J 1986 *Phys. Rev.* B **34** 1835
[20] van Megen W 1995 *Transp. Theory Stat. Phys.* **24** 1017
[21] Chang I and Sillescu H 1997 *J. Phys. Chem.* **101** 8794
[22] Rössler E 1990 *Phys. Rev. Lett.* **65** 1595
[23] Bosse J and Thakur J S 1987 *Phys. Rev. Lett.* **59** 998
[24] Bosse J and Kaneko Y 1995 *Phys. Rev. Lett.* **74** 4023
[25] Schilling R and Scheidsteger T 1997 *Phys. Rev.* E **56** 2932
[26] Fabbian L *et al* 1999 *Phys. Rev.* E **60** 5768
[27] Franosch T *et al* 1997 *Phys. Rev.* E **56** 5659
[28] Götze W, Singh A P and Voigtmann T 2000 *Phys. Rev.* E **61** 6934
[29] Götze W 1984 *Z. Phys.* B **56** 139
[30] Bengtzelius U, Götze W and Sjölander A 1984 *J. Phys. C: Solid State Phys.* **17** 5915
[31] Sjögren L 1986 *Phys. Rev.* A **33** 1254
[32] Alba-Simionesco C and Krauzman M 1995 *J. Chem. Phys.* **102** 6574
[33] Krakoviack V, Alba-Simionesco C and Krauzman M 1997 *J. Chem. Phys.* **107** 3417
[34] Franosch T, Götze W, Mayr M and Singh A P 1997 *Phys. Rev.* E **55** 3183
[35] Götze W and Voigtmann T 2000 *Phys. Rev.* E **61** 4133
[36] Krakoviack V and Alba-Simionesco C 2002 *J. Chem. Phys.* (*Preprint* cond-mat/0204224)
[37] Wuttke J *et al* 2000 *Phys. Rev.* E **61** 2730
[38] Goldammer M *et al* 2001 *Phys. Rev.* E **64** 021303
[39] Surovtsev N V *et al* 1998 *Phys. Rev.* B **58** 14 888
[40] Gapinski J *et al* 1999 *J. Chem. Phys.* **110** 2312
[41] Barshilia H C, Li G, Shen G Q and Cummins H Z 1999 *Phys. Rev.* E **59** 5625
[42] Wuttke J *et al* 1994 *Phys. Rev. Lett.* **72** 3052
[43] Toulouse J, Pick R and Dreyfus C 1996 *Mat. Res. Soc. Symp. Proc.* **407** 161
[44] Wuttke J *et al* 1998 *Eur. Phys. J.* B **1** 169
[45] Shen G Q *et al* 2000 *Phys. Rev.* E **62** 783
[46] Aouadi A *et al* 1997 *J. Phys.: Condens. Matter* **9** 3803
[47] Tao N J, Li G and Cummins H Z 1991 *Phys. Rev. Lett.* **66** 1334
[48] Andrussow L 1969 *Eigenschaften der Materie in ihren Aggregatzuständen: Transportphänomene I* (Landolt–Börnstein II5a) 6th edn (Berlin: Springer)
[49] Wuttke J, Pouget S and Petry W 1996 *J. Chem. Phys.* **105** 5177
[50] Singh A P 1995 *Diplomarbeit* Technische Universität München
[51] Götze W 1996 *J. Stat. Phys.* **83** 1183
[52] Voigtmann T 1998 *Diplomarbeit* Technische Universität München
[53] Cummins H Z *et al* 1997 *Z. Phys.* B **103** 501
[54] Wahnström G and Sjögren L 1982 *J. Phys. C: Solid State Phys.* **15** 401
[55] Morkel C and Gläser W 1986 *Phys. Rev.* A **33** 3383
[56] Leutheusser E 1984 *Phys. Rev.* A **29** 2765